

Constraints on Hidden Sectors Using Rare Kaon Decays

D. Cogollo,^{1,2} M. J. Neves,³ T ssio B. de Melo,^{4,5} Alvaro S. de Jesus,^{6,7} Y. M. Oviedo-Torres,^{8,7} and F. S. Queiroz^{4,8,7,*}

¹*Departamento de F sica, Universidade Federal de Campina Grande, Campina Grande, PB, Brazil*

²*Northwestern University, Department of Physics and Astronomy, 2145 Sheridan Road, Evanston, IL 60208, USA*

³*Departamento de F sica, Universidade Federal Rural do Rio de Janeiro, BR 465-07, 23890-971, Serop dica, RJ, Brazil*

⁴*Millennium Institute for Subatomic Physics at High-Energy Frontier (SAPHIR), Fernandez Concha 700, Santiago, Chile*

⁵*Departamento de Ciencias F sicas, Universidad Andr s Bello, Sazi  2212, Piso 7, Santiago, Chile*

⁶*Departamento de F sica, Universidade Federal do Rio Grande do Norte, 59078-970, Natal, RN, Brasil*

⁷*International Institute of Physics, Universidade Federal do Rio Grande do Norte, 59078-970, Natal, RN, Brasil*

⁸*Departamento de F sica, Universidade Federal da Para ba, Caixa Postal 5008, 58051-970 Jo o Pessoa, PB, Brasil*

The charged Kaon meson (K^+) features several hadronic decay modes, but the most relevant contribution to its decay width stems from the leptonic decay $K^+ \rightarrow \mu^+ \nu_\mu$. Given the precision acquired on the rare decay mode $K^+ \rightarrow \mu^+ \nu_\mu + X$, one can use the data to set constraints on sub-GeV hidden sectors featuring light species that could contribute to it. Light gauge bosons that couple to muons could give rise to sizeable contributions. In this work, we will use data from the $K^+ \rightarrow \mu^+ \nu_\mu l^+ l^-$, and $K^+ \rightarrow \mu^+ \nu_\mu \nu \bar{\nu}$ decays to place limits on light vector bosons present in Two Higgs Doublet Models (2HDM) augmented by an Abelian gauge symmetry, 2HDM- $U(1)_X$. We put our findings into perspective with collider bounds, atomic parity violation, neutrino-electron scattering, and polarized electron scattering probes to show that rare Kaon decays provide competitive bounds in the sub-GeV mass range for different values of $\tan \beta$.

I. INTRODUCTION

The discovery of the Higgs boson announced by ATLAS and CMS collaborations [1, 2] in 2012, and a multitude of flavor physics and electroweak tests attesting the Standard Model (SM) predictions [3–7] have placed severe constraints in extended scalar sectors. The ρ parameter plays an important role in this regard. Two Higgs Doublet Models (2HDM) [8–13] do not alter the ρ parameter because the scalar doublets have hypercharge ± 1 [14], but they are still amenable to flavor physics data. There are several versions of 2HDM and they change according to the Yukawa lagrangian, where one decides whether and how the second Higgs doublet contributes to fermion masses [15]. Several phenomenological studies related to the vacuum stability [16–23], collider physics [24–28], and flavor physics [29, 30] have been done to explore the viable parameter space of such models. In particular, 2HDM are plagued with flavor-changing neutral interactions that severely restrict the viable parameter space of the model. To remedy this issue, discrete symmetries have been invoked in the scalar sector, preventing the appearance of non-diagonal coupling with the scalars [15]. Instead of invoking arbitrary discrete symmetries to justify the contribution of only one scalar doublet to fermions masses, Abelian gauge symmetries stand as more elegant solutions. Abelian symmetries have been studied in the context of 2HDM [31–39]. In [31–33] they are conceived to precisely solve this flavor-changing neutral current problem. In [38] these flavor-changing neutral current problem was resolved and neutrino masses via a type-I seesaw mechanism were incorporated. In [39], the type II seesaw and other possibilities were investigated. Several other phenomenological studies have been conducted in these

2HDM- $U(1)_X$ models addressing the muon anomalous magnetic moment [29, 40], electron-neutrino scattering [41], and dark matter [42, 43].

That said, in this work, we concentrate on models that can free 2HDM from flavor-changing interactions and generate neutrino masses at the same time via the introduction of a new $U(1)_X$ gauge symmetry which is non-anomalous due to the presence of three right-handed neutrinos. The absence of flavor-changing interactions is addressed by properly assigning different quantum numbers to the two Higgs doublets. In this way, only one of the Higgs doublet contributes to fermion masses. The right-neutrinos acquire a Majorana mass term after the spontaneous symmetry breaking of the $U(1)_X$ gauge symmetry that leads to a type I seesaw mechanism due to a Dirac mass term involving the active neutrinos [44–48]. The breaking of the $U(1)_X$ gauge symmetry gives rise to a hidden sector comprised of dark higgs and a vector boson. The mass of the vector boson will be proportional to the vacuum expectation value of the $U(1)_X$ breaking and the gauge couplings of the $U(1)_X$ gauge symmetry.

In principle, such 2HDM- $U(1)_X$ models can host sub-GeV hidden sectors that are entitled to an interesting phenomenology. Having in mind the historical importance of the Kaon meson to the construction of the Standard Model since its discovery in 1947 and the precision acquired in the measurement of its rare decays, several works have been put forth assessing their potential to probe hidden sectors [49–53]. In our work, we will focus on the sub-GeV vector boson contribution to the rare decays $K^+ \rightarrow \mu^+ \nu_\mu e^- e^+$ and $K^+ \mu^+ \nu_\mu \nu \nu$ in the context of 2HDM- $U(1)_X$. As we have a concrete and well-motivated model at hand, several phenomenological studies have been carried out in the past. Thus, we put our findings into perspective with collider bounds, atomic parity violation, neutrino-electron scattering, and polarized electron scattering probes to show that the K^+ meson offers an orthogonal and complementary probe to such hidden sectors.

* farinaldo.queiroz@ufrn.br

The paper is organized as follows. In the Section II, we present the structure of the 2HDM models with the extra group $U(1)_X$ such as the particle content. The section III is dedicated to gauge bosons masses in the scenario of a light Z' and the correspondent couplings with the fermions of the particle content, relegating the detailed coupling expressions of the results to the Appendix VII. In Section IV, we present the existing constraints on the model based on accelerators, polarized electron scattering, and neutrino-electron scattering. The section V, we derive bounds on hidden vectors using rare K^+ decays. In the section VI, we discuss the final remarks and conclusions.

II. THE 2HDM – $U(1)_X$ MODEL

Two Higgs Doublet Models (2HDM) augmented by an abelian gauge symmetry, 2HDM- $U(1)_X$, are constructed as symmetric lagrangians under transformations of the gauge group $\mathcal{G}_{2HDMX} \equiv SU(3)_c \times SU(2)_L \times U(1)_Y \times U(1)_X$. As aforementioned, scalar doublets with hypercharge $Y = \pm 1$, or scalar singlets with $Y = 0$, do not modify the ρ parameter, this allows us to work with a family of models featuring two scalar doublets, Φ_1 and Φ_2 , along with a scalar singlet Φ_s , whose scalar potential is given by:

$$\begin{aligned} V(\Phi_1, \Phi_2, \Phi_s) &= m_1^2 (\Phi_1^\dagger \Phi_1) + m_2^2 (\Phi_2^\dagger \Phi_2) + m_s^2 (\Phi_s^\dagger \Phi_s) \\ &+ \frac{\lambda_1}{2} (\Phi_1^\dagger \Phi_1)^2 + \frac{\lambda_2}{2} (\Phi_2^\dagger \Phi_2)^2 + \frac{\lambda_s}{2} (\Phi_s^\dagger \Phi_s)^2 \\ &+ \lambda_3 (\Phi_1^\dagger \Phi_1) (\Phi_2^\dagger \Phi_2) + \lambda_4 (\Phi_1^\dagger \Phi_2) (\Phi_2^\dagger \Phi_1) \\ &+ \mu_1 (\Phi_1^\dagger \Phi_1) (\Phi_s^\dagger \Phi_s) + \mu_2 (\Phi_2^\dagger \Phi_2) (\Phi_s^\dagger \Phi_s) \\ &+ \mu \Phi_1^\dagger \Phi_2 \Phi_s + \text{h. c.}, \end{aligned} \quad (1)$$

where the parameters m_i ($i = 1, 2$), λ_i ($i = 1, 2, 3, 4$), m_s , λ_s , μ_i ($i = 1, 2$) and μ , will be considered to be real. To avoid flavor-changing neutral interactions, all charged fermions stem from a Yukawa lagrangian where just the Φ_2 doublet couples to the fermion fields,

$$-\mathcal{L}_{Y_{2HDM}} = y_{i,j}^d \bar{Q}_{iL} \Phi_2 d_{jR} + y_{i,j}^u \bar{Q}_{iL} \tilde{\Phi}_2 u_{jR} + y_{i,j}^e \bar{L}_{iL} \Phi_2 e_{jR} + \text{h.c.}, \quad (2)$$

being $i, j = 1, 2, 3$ a family index, $L_{iL} = (\nu_{iL} \ e_{iL})^T$ left-handed doublets of leptons, e_{iR} right-handed singlets of charged leptons, $Q_{iL} = (u_{iL} \ d_{iL})^T$ left-handed doublets of quarks, u_{iR} , d_{iR} right-handed singlets of quarks, and $\tilde{\Phi}_2$ a scalar doublet defined as $\tilde{\Phi}_2 = i \sigma_2 \Phi_2^*$. As for neutrinos, their masses come from a type I seesaw mechanism implemented in a Yukawa lagrangian that involves the Φ_2 doublet, the Φ_s singlet, and the presence of right-handed neutrinos (N_R):

$$-\mathcal{L} \supset y_{ij}^D \bar{L}_{iL} \tilde{\Phi}_2 N_{jR} + Y_{ij}^M \overline{(N_{iR})^c} \Phi_s N_{Rj}. \quad (3)$$

The three copies of right-handed neutrinos were introduced to generate neutrino masses and to free the model from gauge anomalies. Setting q_{Φ_1} , q_{Φ_2} , q_{Φ_s} as the $U(1)_X$ charges of the scalar doublets and the scalar singlet, respectively, we notice

that these charges obey the relations, $q_{\Phi_1} \neq q_{\Phi_2}$, and $q_{\Phi_s} = q_{\Phi_1} - q_{\Phi_2}$ with $u \neq -2d$ (see text in the table I for more details about the u and d charges).

After the spontaneous symmetry breaking process, the scalar fields can be parameterized as usual:

$$\Phi_i = \begin{pmatrix} \phi_i^+ \\ (v_i + \rho_i + i\eta_i) / \sqrt{2} \end{pmatrix}, \quad (4)$$

$$\Phi_s = \frac{1}{\sqrt{2}} (v_s + \rho_s + i\eta_s), \quad (5)$$

and the charged fermions will gain Dirac masses from (2), whereas the neutrinos will gain masses through the type I seesaw mechanism from (3),

$$\mathcal{L}_{mass}^{\nu N} = (\nu \ N) \begin{pmatrix} 0 & m_D \\ m_D^T & M_R \end{pmatrix} \begin{pmatrix} \nu \\ N \end{pmatrix}. \quad (6)$$

In the case for when $M_R \gg m_D$, being $m_D = \frac{y^D v_2}{2\sqrt{2}}$ and $M_R = \frac{y^M v_s}{2\sqrt{2}}$, it is obtained the usual light neutrino mass matrix $m_\nu = -m_D^T \frac{1}{M_R} m_D$, and the usual heavy neutrino mass matrix $m_N = M_R$. We will assume throughout that the Yukawa couplings y^M are larger enough to generate right-handed neutrino masses greater than $M_{Z'}$, avoiding Z' decay into these RHN. This assumption guarantees that the Z' decays are into SM fermions.

In order to compute the hidden boson contribution to the K^+ decay, we will obtain in the next section the couplings among the Z' boson and fermions for these families of models featuring two scalar doublets, Φ_1 and Φ_2 , along with a scalar singlet Φ_s .

III. THE GAUGE BOSONS MASSES AND COUPLINGS

The gauge boson masses rise from the kinetic terms of the scalar fields. To derive them, we need to correctly write the covariant derivative. The presence of a new $U(1)_X$ symmetry implies that the covariant derivative is,

$$D_\mu = \partial_\mu + i g T^a W_{a\mu} + i g' \frac{Q_Y}{2} \hat{B}_\mu + i g_X \frac{q_X}{2} \hat{X}_\mu, \quad (7)$$

where g , g' and g_X are the dimensionless coupling constants of the $SU(2)_L$, $U(1)_Y$, $U(1)_X$ gauge groups respectively, $W_{a\mu}$ and $T^a = \sigma^a / 2$ ($a = 1, 2, 3$) are the gauge bosons and generators of the $SU(2)_L$ group, \hat{B}_μ and \hat{X}_μ are gauge bosons of the $U(1)_Y$ and $U(1)_X$ groups respectively, Q_Y (hypercharge), and q_X are the charges associated to the groups $U(1)_Y$ and $U(1)_X$, respectively. The kinetic terms of the gauge bosons are [54–56],

$$\mathcal{L}_{\text{gauge}} = -\frac{1}{4} \hat{B}_{\mu\nu} \hat{B}^{\mu\nu} + \frac{\epsilon}{2 \cos\theta_W} \hat{X}_{\mu\nu} \hat{B}^{\mu\nu} - \frac{1}{4} \hat{X}_{\mu\nu} \hat{X}^{\mu\nu}. \quad (8)$$

The kinetic mixing between the two Abelian groups should fulfill $\epsilon \ll 1$ to be consistent with electroweak constraints. It

	$U(1)_X$	$U(1)_A$	$U(1)_B$	$U(1)_C$	$U(1)_D$	$U(1)_E$	$U(1)_F$	$U(1)_G$	$U(1)_{B-L}$
L_{iL}	$-\frac{3}{2}(u+d)$	0	0	$+3/4$	$-3/2$	$-3/2$	-3	$-1/2$	-1
e_{iR}	$-2u-d$	-1	+1	0	-2	-1	$-10/3$	0	-1
N_{iR}	$-u-2d$	+1	-1	$+3/2$	-1	-2	$-8/3$	-1	-1
Q_{iL}	$\frac{u+d}{2}$	0	0	$-1/4$	$+1/2$	$+1/2$	+1	$+1/6$	$+1/3$
u_{iR}	u	+1	-1	$+1/2$	+1	0	$+4/3$	$-1/3$	$+1/3$
d_{iR}	d	-1	+1	-1	0	+1	$+2/3$	$+2/3$	$+1/3$
Φ_1	$\frac{5u}{2} + \frac{7d}{2}$	-1	+1	$-9/4$	$+5/2$	$+7/2$	$+17/3$	$+3/2$	+2
Φ_2	$\frac{u-d}{2}$	+1	-1	$+3/4$	$+1/2$	$-1/2$	$+1/3$	$-1/2$	0
Φ_s	$2u+4d$	-2	+2	-3	+2	+3	$+16/3$	+2	+2

Table I. $U(1)_X$ charges of the particles in the models. We assign a charge $q = u$ and $q = d$ for the down quarks and derive all remaining $U(1)_X$ charges by requiring that the model is free from gauge anomalies and that Eqs.(2)-(3) are satisfied.

can be removed through the redefinition $\hat{B}_\mu = \eta_X X_\mu + B_\mu$ and $\hat{X}_\mu = X_\mu$ with,

$$\eta_X = \frac{\epsilon / \cos \theta_W}{\sqrt{1 - (\epsilon / \cos \theta_W)^2}} \simeq \frac{\epsilon}{\cos \theta_W}. \quad (9)$$

After that, the derivative covariant operator reads,

$$D_\mu = \partial_\mu + i g \frac{\sigma_a}{2} W_{a\mu} + i g' \frac{Q_Y}{2} B_\mu + \frac{i}{2} G_{X_i} X_\mu, \quad (10)$$

where $G_{X_i} = g_X q_{X_i} + \epsilon g' Q_Y / \cos \theta_W$, with X_i being the field in question. Thus, for the scalar doublets we get $G_{X_1} = g_X q_{\Phi_1} + \epsilon g' Q_Y / \cos \theta_W$, $G_{X_2} = g_X q_{\Phi_2} + \epsilon g' Q_Y / \cos \theta_W$. Applying the covariant derivative Eq.(10) into the kinetic Lagrangian:

$$\mathcal{L}_{Kinetic} = |D_\mu \Phi_1|^2 + |D_\mu \Phi_2|^2 + |D_\mu \Phi_s|^2, \quad (11)$$

and using the scalar fields in Eq.(4)-(5) we get,

$$\mathcal{L}_{mass} = \frac{v^2}{8} (g^2 W_{3\mu} W_3^\mu - 2g g' W_{3\mu} B^\mu + g'^2 B_\mu^2) + \frac{1}{2} \left[m_X^2 X_\mu^2 - 2 \frac{g}{g_Z} \Delta^2 W_{3\mu} X^\mu + 2 \frac{g'}{g_Z} \Delta^2 B_\mu X^\mu \right], \quad (12)$$

where $m_X^2 = (G_{X_1}^2 v_1^2 + G_{X_2}^2 v_2^2 + g_X^2 q_{\Phi_s}^2 v_s^2)/4$, and we have defined $\Delta^2 = g_Z (G_{X_1} v_1^2 + G_{X_2} v_2^2)/4$ and $g_Z = \sqrt{g^2 + g'^2}$. A first diagonalization process is carried out through the well-known electroweak rotation,

$$\begin{aligned} B_\mu &= \cos \theta_W A_\mu - \sin \theta_W Z_\mu^0 \\ W_\mu^3 &= \sin \theta_W A_\mu + \cos \theta_W Z_\mu^0, \end{aligned} \quad (13)$$

where θ_W is the Weinberg angle that satisfies the relations $e = g \sin \theta_W = g' \cos \theta_W$. After the rotation (13), the field A_μ is identified as the massless photon, as it must be, and the Lagrangian (12) is reduced to,

$$\mathcal{L}_{mass} = \frac{1}{2} m_{Z^0}^2 Z_\mu^0 Z^{0\mu} - \Delta^2 Z_\mu^0 X^\mu + \frac{1}{2} m_X^2 X_\mu X^\mu, \quad (14)$$

where $m_{Z^0}^2 = g_Z^2 v^2/4$, with $g_Z = g/\cos \theta_W$ and $v^2 = v_1^2 + v_2^2$. The Z^0 boson with its usual mass was nicely recovered, but there is still mixing between Z_μ^0 and X_μ . We call

the attention that the mixing between these two bosons depends on Δ^2 and consequently on the $U(1)_X$ charges of the scalar doublets. The diagonalization of Eq.(14) is carried out through the rotation,

$$\begin{pmatrix} Z'_\mu \\ X'_\mu \end{pmatrix} = \begin{pmatrix} \cos \xi & -\sin \xi \\ \sin \xi & \cos \xi \end{pmatrix} \begin{pmatrix} Z_\mu^0 \\ X_\mu \end{pmatrix}, \quad (15)$$

with,

$$\tan(2\xi) = \frac{2\Delta^2}{m_{Z^0}^2 - m_X^2}, \quad (16)$$

and a new pair of eigenvalues,

$$\begin{aligned} M_Z^2 &= \frac{1}{2} \left[m_{Z^0}^2 + m_X^2 + \sqrt{(m_{Z^0}^2 - m_X^2)^2 + 4(\Delta^2)^2} \right], \\ M_{Z'}^2 &= \frac{1}{2} \left[m_{Z^0}^2 + m_X^2 - \sqrt{(m_{Z^0}^2 - m_X^2)^2 + 4(\Delta^2)^2} \right]. \end{aligned} \quad (17)$$

As we said, we are interested in studying the case for when the Z' -gauge boson is lighter than the Z -boson. In this regime, the mixing angle Eq.(16) can be approximated to,

$$\xi \simeq \frac{\Delta^2}{m_Z^2} = \frac{1}{g_Z} (G_{X_1} \cos^2 \beta + G_{X_2} \sin^2 \beta), \quad (18)$$

which simplifies to,

$$\xi \simeq \epsilon_Z + \epsilon \tan \theta_W, \quad (19)$$

where,

$$\epsilon_Z = \frac{g_X}{g_Z} (q_{\Phi_1} \cos^2 \beta + q_{\Phi_2} \sin^2 \beta). \quad (20)$$

Using this small mixing approximation the eigenvalues (17) reduce to,

$$\begin{aligned} M_Z^2 &\simeq \frac{1}{4} g_Z^2 v^2, \\ M_{Z'}^2 &\simeq \frac{1}{2} g_X |q_{\Phi_s}| \sqrt{v_s^2 + v^2 \sin^2 \beta \cos^2 \beta}. \end{aligned} \quad (21)$$

where we have used the common parameterization of the vacuums with $v_1 = v \cos \beta$, and $v_2 = v \sin \beta$, such that

$\tan \beta = v_2/v_1$. Realize that $M_{Z'}$ in Eq.(21) depends on the free parameters g_X , v_s , β and the $U(1)_X$ charge of the singlet scalar.

We have derived the physical gauge bosons, their masses and the relevant mixings. These quantities are key to our findings, which are governed by the neutral current of the hidden vector boson. The full calculation of this neutral current is presented in the Appendix VII, as well as the neutral current mediated by the standard Z boson. For now, we just show here the general expression we used to derive our results,

$$\mathcal{L}_{Z'}^{int} = g_V^{(\Psi_i)} \bar{\Psi}_i \not{Z}' \Psi_i + g_A^{(\Psi_i)} \bar{\Psi}_i \not{Z}' \gamma_5 \Psi_i, \quad (22)$$

being Ψ_i each one of the fermions of the SM, g^V and g^A the vector and axial factors whose explicit forms are presented in the Appendix VII

IV. EXISTING CONSTRAINTS

In this section, we discuss the existing bounds for the region of interest, namely $10 \text{ MeV} < M_{Z'} < 200 \text{ MeV}$. We will discuss collider limits, polarized electron scattering, and neutrino-electron scattering. We start with collider searches for charged scalars which turn out to be the most relevant one.

A. Collider Bounds on Charged Scalars

An important bound rises from charged Higgs boson searches, H^\pm . The most relevant bound in our work is the one derived from LEP data, which has presented a lower bound on M_{H^\pm} ($M_{H^\pm} > 80 \text{ GeV}$ for $\tan \beta \geq 10$) for a Type-I 2HDM charged Higgs boson H^\pm [57]. For the family of $SU(2)_L \times U(1)_Y \times U(1)_X$ 2HDM extensions of the Standard Model we are studying here, M_{H^\pm} is given by [58],

$$M_{H^\pm}^2 = \left(\sqrt{2} \mu v_s - \lambda_4 v_1 v_2 \right) \frac{v^2}{2v_1 v_2} \quad (23)$$

which implies that,

$$M_{H^\pm}^2 = \frac{\sqrt{2} \mu v_s - \lambda_4 v^2 \sin \beta \cos \beta}{2 \sin \beta \cos \beta}, \quad (24)$$

depending on the β -parameter, the VEV v_s of the singlet scalar, as well as the parameters μ and λ_4 present in the scalar potential of the model, Eq.(1). For the parameters μ and λ_4 of the scalar potential, we must be careful in order to avoid an imaginary M_{H^\pm} value, and perturbativity violation, respectively. Doing so, we assumed reasonable values for these parameters in our calculations, with $\mu = 100 \text{ GeV}$ (μ is only bounded from below) and $\lambda_4 = 0.1$ (λ_4 parameter only being bounded from above). We performed our analysis for two different values of $\tan \beta$, $\tan \beta = 10$ and $\tan \beta = 50$. After setting these values of $\tan \beta$, M_{H^\pm} in Eq.(24) depends just on v_s . The recast of this bound on the $g_X, M_{Z'}$ plane is made by exploring the mutual dependence of the mass of the

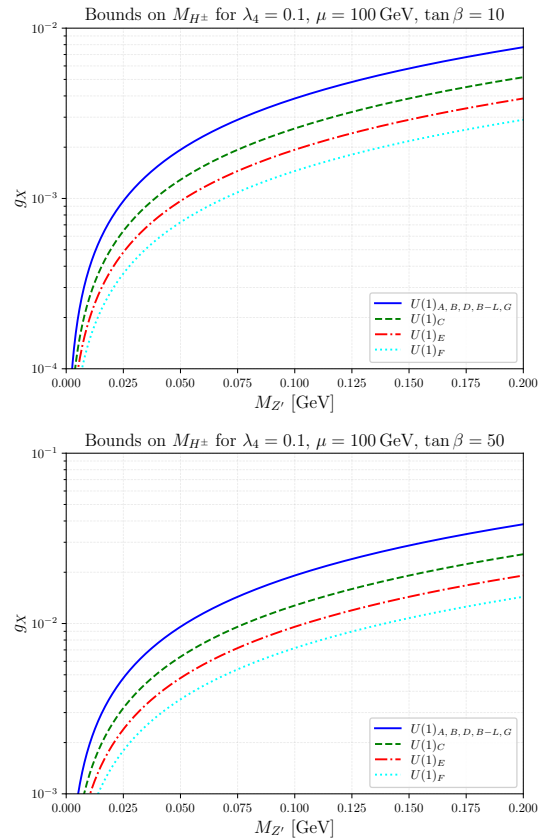


Figure 1. Summary of the limits for all of the models in the $g_X \times m_{Z'}$ parameter space coming from the experimental limits on the mass of the charged Higgs H^\pm searches at LEP.

charged Higgs and Z' with the free parameter v_s , as seen in Eq.(21) and Eq.(24). Being q_{Φ_s} the scalar singlet charge under $U(1)_X$, and as $M_{Z'}$ depends on $|q_{\Phi_s}|$, this bound becomes model-dependent, as it can be seen in Figure (1) for the cases of $\tan \beta = 10$ (top) and $\tan \beta = 50$ (bottom), with the area above the lines being excluded since they represent a region of the parameter space where the mass of the charged Higgs is below the bound from LEP. There is a similarity among the bounds of the models $U(1)_A$, $U(1)_B$, $U(1)_D$, $U(1)_{B-L}$ and $U(1)_G$, which comes from the fact that these models have $|q_{\Phi_s}| = 2$, while the models $U(1)_C$, $U(1)_E$, and $U(1)_F$ show stronger bounds due to larger values of $|q_{\Phi_s}|$.

B. Polarized Electron Scattering

Low energy polarized electron scattering offers an orthogonal probe to light hidden particles that feature kinetic and mass mixing with the Z boson. In other words, the weak currents in the presence of such mass mixings and kinetic mixings can be parameterized in terms of a shift in the Weinberg angle as follows [41],

$$\Delta \sin^2 \theta_W \simeq -0.42 \epsilon \delta \frac{m_Z}{m_{Z'}} f(Q^2/m_{Z'}^2), \quad (25)$$

where $f(Q^2/m_{Z'}^2)$ is the propagator function [41] with the masses and the energy Q in MeV units. δ is the mass mixing parameter defined as,

$$\delta = \frac{m_Z}{m_{Z'}} \epsilon_Z. \quad (26)$$

Thus, if we happen to measure the Weinberg angle at a given energy Q , we can limit the contribution of new physics to $\sin^2 \theta_W$ as a function of δ and ϵ with,

$$\epsilon^2 \simeq \frac{5.7}{\delta^2} (\Delta \sin^2 \theta_W)^2 \left(\frac{m_{Z'}^2 + Q^2}{m_Z m_{Z'}} \right)^2. \quad (27)$$

The E158 experiment measured $\sin^2 \theta_W = 0.2329(13)$ with $Q = 160$ MeV [59], which leads to,

$$\epsilon^2 < \frac{1.5 \times 10^{-5}}{\delta^2} \left(\frac{m_{Z'}^2 + 160^2}{m_Z m_{Z'}} \right)^2. \quad (28)$$

For the $U(1)_{B-L}$ model $\epsilon_Z = 2g_X \cos^2 \beta / g_Z$. Consequently,

$$\epsilon < 1.8 \times 10^{-5} / g_X, \quad (29)$$

for $m_{Z'} \sim 100$ MeV, which is the region of interest here. A similar relation can be derived for the other models. The bounds arising from rare Kaon decay will lie in the range of $g_X \sim 10^{-2} - 10^{-3}$, we assume the kinetic mixing to be sufficiently small ($\epsilon \sim 10^{-4}$) to be consistent with polarized electron scattering measurements.

C. Neutrino-Electron Scattering

Hidden particles can contribute to neutrino-electron scattering. Using data from TEXONO, CHARM-II and GEMMA collaborations, one can compute the neutrino-electron scattering cross section given by,

$$\frac{d\sigma}{dT}(\bar{\nu}e \rightarrow \bar{\nu}e) = \frac{m_e G_F^2}{4\pi} \left[g_1^2 + g_2^2 \left(1 - \frac{T}{E_\nu} \right)^2 - g_1 g_2 \frac{m_e T}{E_\nu^2} \right], \quad (30)$$

where E_ν and T are the neutrino energy and electron recoil energy, respectively. A similar cross-section exists for $\nu e \rightarrow \nu e$ scattering, and the scattering cross-section is equal to Eq.(30), by interchanging g_1 and g_2 . The couplings $g_{1,2}$ encode all the coupling constants involved in the SM and Z' interactions. For heavy hidden vectors with masses larger than 1.5 GeV, the neutrino-electron scattering can be described in terms of effective operators. The strongest constraint in this case arises from CHARM-II, which features the best precision. For hidden vectors with masses between 400 keV and 1.5 GeV a trade-off between energy threshold and precision takes place. Considering data from GEMMA, TEXONO, and CHARM-II that cover various energy scales, constraints on the kinetic mixing parameter were derived from several vector bosons [60]. In particular, for $M_{Z'} = 1$ MeV, we need to impose $\epsilon < 10^{-4}$, whereas for $M_{Z'} = 100$ MeV, we require $\epsilon < 10^{-3}$. In our

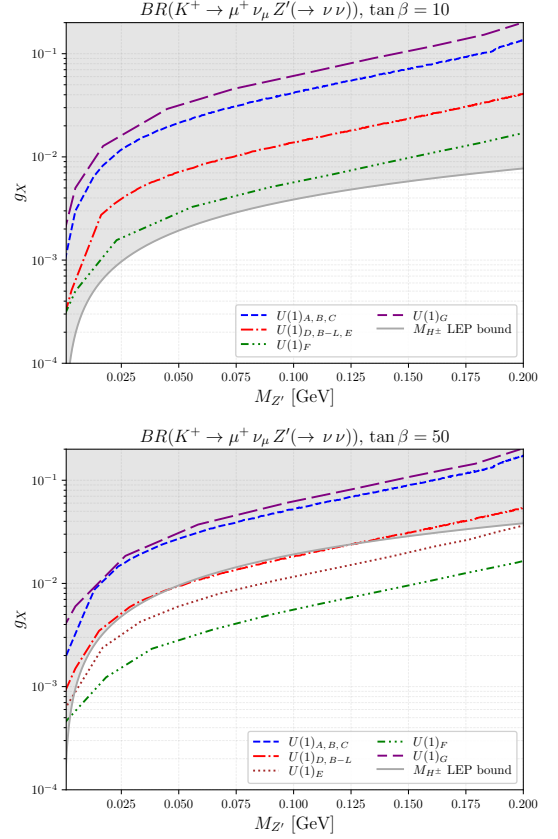


Figure 2. Bounds on g_X as a function of the hidden vector mass for $\tan \beta = 10$ and $\tan \beta = 50$, respectively, using the K^+ decay into $\mu^+ \nu_\mu \bar{\nu} \nu$. The LEP bound delimited by a grey region stems from charged scalar searches. As the charged scalar mass is related to $\tan \beta$, the LEP bound changes for different values of $\tan \beta$. From the plots, we conclude that K^+ decays yield competitive limits, especially for $\tan \beta = 50$.

work, we are focusing on $10 \text{ MeV} < M_{Z'} < 200 \text{ MeV}$, thus we safely obey these limits by assuming $\epsilon = 10^{-4}$. We have checked that values of $\epsilon \ll 10^{-4}$ yield no meaningful change in our results.

Taking into account three different sources of constraints, we conclude that the neutrino-electron scattering and collider searches for charged scalars provide the most restrictive bound in our model. The latter will be shown in our figures, whereas the former is obeyed by assuming $\epsilon = 10^{-4}$ throughout.

In summary, we have reviewed different constraints that are relevant to our model, and concluded that as long as we keep the kinetic mixing to be $\epsilon = 10^{-4}$, the bound on the charged scalar rising from LEP data ends up being the most relevant for our reasoning.

V. BOUNDS FROM RARE K^+ DECAYS

Rare decays of the K^+ meson can be considered as radiative corrections to its main decay mode $K^+ \rightarrow \mu^+ \nu_\mu$, when

from the muon leg is radiate a light Z' boson that subsequently decay into $Z' \rightarrow e^- e^+$ or $Z' \rightarrow \bar{\nu} \nu$. In both cases the first information we should get is the width of the decay mode $K^+ \rightarrow \mu^+ \nu_\mu Z'$. Recently, it was shown in [61] that its analytical expression is given by,

$$\Gamma(K^+ \rightarrow \mu^+ \nu_\mu Z') = \frac{1}{64\pi^3 M_K} \int_{E_{min}}^{E_{max}} \sum_{spins} |\mathcal{M}|^2 dE_\nu dE_\mu, \quad (31)$$

where $|\mathcal{M}|^2$ is the square of the invariant amplitude of the process and $M_K = 493.677$ MeV is the mass of the meson K^+ . The limits of the integration are written as,

$$\begin{aligned} E_\mu^{min} &= m_\mu, \\ E_\mu^{max} &= \frac{M_K^2 + m_\mu^2 - M_{Z'}^2}{2M_K}, \\ E_\nu^{min} &= \frac{M_K^2 + m_\mu^2 - M_{Z'}^2 - 2M_K E_\mu}{2(M_K - E_\mu + \sqrt{E_\mu^2 - m_\mu^2})}, \\ E_\nu^{max} &= \frac{M_K^2 + m_\mu^2 - M_{Z'}^2 - 2M_K E_\mu}{2(M_K - E_\mu - \sqrt{E_\mu^2 - m_\mu^2})}, \end{aligned} \quad (32)$$

in which $m_\mu = 105.66$ MeV is the mass of the muon, E_μ is the energy in the final state of the muon, constrained by the condition $E_\mu \geq m_\mu$, and E_ν is the energy of the outgoing neutrino, bounded by kinematic conditions. The full expression of $|\mathcal{M}|^2$ in Eq.(31) is [61],

$$\begin{aligned} \sum_{spins} |\mathcal{M}|^2 &= \frac{G_F^2 f_K^2 |V_{us}|^2}{M_{Z'}^2 (Q^2 - m_\mu^2)^2} [g_L^2 Q^4 (2E_\mu M_K (M_{Z'}^2 + m_\mu^2 - Q^2) - 2E_{Z'} M_K M_{Z'}^2) \\ &\quad - M_K^2 m_\mu^2 + M_K^2 Q^2 - m_\mu^4 + m_\mu^2 Q^2 + 2M_{Z'}^4 - m_\mu^2 M_{Z'}^2 - M_{Z'}^2 Q^2) \\ &\quad + 6g_L g_R m_\mu^2 M_{Z'}^2 Q^2 (Q^2 - M_K^2) + g_R^2 m_\mu^2 (-2E_\mu M_K^3 (M_{Z'}^2 + m_\mu^2 - Q^2) \\ &\quad + 2E_{Z'} (E_\nu M_{Z'}^2 (M_K^2 - Q^2) + M_K^3 (Q^2 - m_\mu^2) + M_K Q^2 (M_{Z'}^2 + m_\mu^2 - Q^2)) \\ &\quad + M_K^4 m_\mu^2 + M_K^4 M_{Z'}^2 - M_K^4 Q^2 + M_K^2 m_\mu^4 - M_K^2 m_\mu^2 Q^2 \\ &\quad - 3M_K^2 M_{Z'}^4 + 2M_K^2 m_\mu^2 M_{Z'}^2 + M_{Z'}^4 Q^2 - m_\mu^2 M_{Z'}^2 Q^2)], \end{aligned} \quad (33)$$

where $g_L = g_V - g_A$ and $g_R = g_V + g_A$ are defined as combinations of the vector (g_V) and axial (g_A) coefficients from Eq.(48), $Q^2 = M_K^2 - 2M_K E_\nu$, $E_{Z'}$ is the energy of the emitted Z' boson, $G_F = 1.166 \times 10^{-5}$ GeV $^{-2}$ is the Fermi constant, $f_K = 155.7$ MeV the Kaon decay constant, and $|V_{us}| = \sin \theta_c = 0.22534$ is the sine of the Cabibbo angle.

A. The $K^+ \rightarrow \mu^+ \nu_\mu Z' (\rightarrow \bar{\nu} \nu)$ decay

NA62 collaboration reported null results for the rare decay $K^+ \rightarrow \mu^+ \nu_\mu \bar{\nu} \nu$, which led to the 90% CL upper limit [62],

$$\mathcal{B}(K^+ \rightarrow \mu^+ \nu_\mu \bar{\nu} \nu) < 1.0 \times 10^{-6}. \quad (34)$$

When Z' is on-shell, we can write Eq.(34) as,

$$\mathcal{B}(K^+ \rightarrow \mu^+ \nu_\mu Z') \cdot \mathcal{B}(Z' \rightarrow \bar{\nu} \nu) < 1.0 \times 10^{-6}, \quad (35)$$

with each one of the branching in Eq.(35) defined as usual,

$$\mathcal{B}(K^+ \rightarrow \mu^+ \nu_\mu Z') = \frac{\Gamma(K^+ \rightarrow \mu^+ \nu_\mu Z')}{\Gamma_{K^+}}, \quad (36a)$$

$$\mathcal{B}(Z' \rightarrow \bar{\nu} \nu) = \frac{\Gamma(Z' \rightarrow \bar{\nu} \nu)}{\Gamma_{Z'}}, \quad (36b)$$

being $\Gamma_{K^+} = 5.38 \times 10^{-17}$ GeV [59] the total decay width of the meson K^+ and $\Gamma_{Z'}$ the total decay width of the Z' boson. The width decay of the Z' boson into any pair of anti-fermion-fermion ($\bar{f} f$) is given by,

$$\begin{aligned} \Gamma_{Z' \rightarrow \bar{f} f} &= \frac{M_{Z'}}{12\pi} N_c^f \sqrt{1 - \frac{4m_f^2}{M_{Z'}^2}} \left[(g_V^f)^2 + (g_A^f)^2 \right. \\ &\quad \left. + \frac{2m_f^2}{M_{Z'}^2} \left((g_V^f)^2 - 2(g_A^f)^2 \right) \right], \end{aligned} \quad (37)$$

where N_c^f is the number of colors of the final state fermion, $N_c^Q = 3$ for quarks, $N_c^\ell = 1$ for charged leptons and neutrinos. The partial width decay Eq.(37) is allowed for when $M_{Z'} > 2m_f$, and the total width decay $\Gamma_{Z'}$ is the sum over each one of the kinematically allowed partial width decay $\Gamma_{Z' \rightarrow \bar{f} f}$ in Eq.(37).

B. The $K^+ \rightarrow \mu^+ \nu_\mu Z' (\rightarrow e^+ e^-)$ decay

However, the search for the rare decay mode of the type $K^+ \rightarrow \mu^+ \nu_\mu e^+ e^-$ resulted in the recent observation of over two thousand events. Hence, instead of an upper limit the

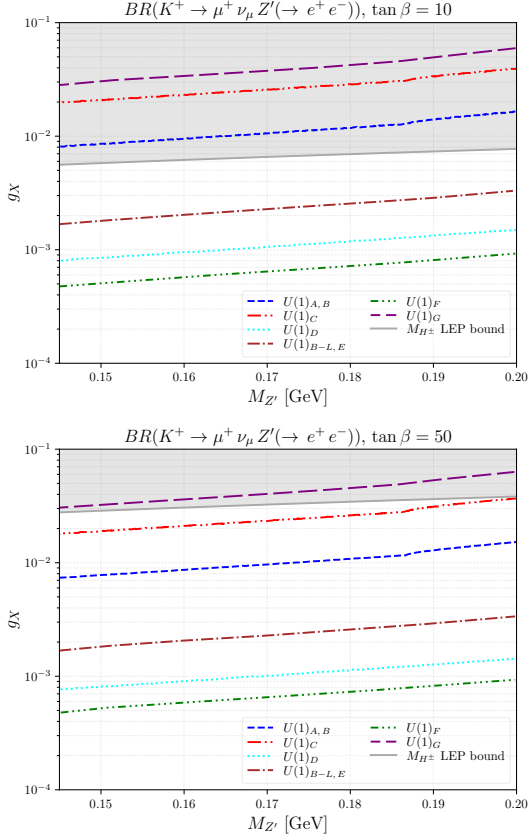


Figure 3. Bounds on the g_X as a function of the hidden vector mass, assuming $\tan\beta = 50$ for different $U(1)_X$ extensions. Our upper limits are represented with dotted and dashed curves. The LEP bound is delimited by the grey region. Therefore, the impressive precision achieved in this decay mode turned it into an excellent laboratory for hidden vector bosons. From the plots, we find that it provides the most constraining bounds for several models for either $\tan\beta = 10$ or $\tan\beta = 50$.

branching ratio was measured to be [63],

$$\mathcal{B}(K^+ \rightarrow \mu^+ \nu_\mu e^- e^+) = (7.06 \pm 0.31) \times 10^{-8}, \quad (38)$$

It is important to point out that Eq.(38) was derived for an invariant electron positron mass $m_{ee} > 145$ MeV. Thus, it applies for $m_{Z'} > 145$ MeV. Expressing the branching ratio as a product of the branchings,

$$\mathcal{B}(K^+ \rightarrow \mu^+ \nu_\mu Z') \cdot \mathcal{B}(Z' \rightarrow e^- e^+) = (7.06 \pm 0.31) \times 10^{-8}, \quad (39)$$

with,

$$\mathcal{B}(Z' \rightarrow e^- e^+) = \frac{\Gamma(Z' \rightarrow e^- e^+)}{\Gamma_{Z'}}, \quad (40)$$

we can place constraints on the properties of the hidden vector.

C. Bounds on Hidden Sectors

We remind the reader that we are interested in deriving bounds on hidden sectors using data from rare K^+ decay. Due

to kinematics, we will focus on the $M_{Z'} = 1 - 200$ MeV mass range. Regarding the possible Z' decays, the Z' may decay into the first generation of leptons and light quarks through Eq.(48). We highlight that the hadronic contributions have been calculated at parton level, and right-handed neutrinos are taken to be heavy, thus not kinematically accessible. As the branching ratios depend on the couplings between the Z' with fermions which in term are governed by $\tan\beta$ and g_X for a given $U(1)_X$ gauge symmetry, we can plot the constraints in the g_X vs $M_{Z'}$ plane. In the Appendix VII, we show the explicit expression of the neutral current.

Therefore, we derive our numerical results for $\tan\beta = 10$ and $\tan\beta = 50$, and overlay our findings with LEP bound on the singly charged scalar discussed previously, which happens to be the most restrictive one as we are assuming the kinetic mixing to be sufficiently suppressed. The LEP bound is delimited by a grey region. In Fig.2 we present our lower bounds on the gauge couplings as a function of the Z' mass based on the $K^+ \rightarrow \mu^+ \nu_\mu Z' (\rightarrow \bar{\nu} \nu)$ decay. In the upper panel, where $\tan\beta = 10$, we clearly see that the search for rare K^+ decays results in limits that are weaker than those from LEP, which refers to $M_{H^\pm} < 80$ GeV. Analyzing the plots, we find that all the $U(1)_X$ models are excluded by LEP for the case of $\tan\beta = 10$, however, increasing the β -parameter for $\tan\beta = 50$, we observe that the models $U(1)_E$ and $U(1)_F$ are not ruled out by the LEP bound, showing that the search for rare meson decays can produce stronger bounds for these models. This happens due to the fact that the LEP bound gets weaker (see Figure 1) while the bounds on $\mathcal{BR}(Z' \rightarrow \nu\nu)$ do not change by much with higher values of $\tan\beta$, with the only exception being the model $U(1)_F$, which presents a change by a factor of 2.

In the bottom panel, with $\tan\beta = 50$, the situation changes significantly though, especially for models in which the invisible decay is large, such as $U(1)_{B-L}, U(1)_E, U(1)_F$, etc. With $\tan\beta = 50$, we impose $g_X < 1 \times 10^{-3}$ for $M_{Z'} \sim 25$ MeV for the $U(1)_F$ model, and $g_X < 5 \times 10^{-3}$ for the $U(1)_{B-L}$ model. We remind the reader that we assumed $\epsilon = 10^{-4}$ throughout, but we have checked that our numerical results will not change by a factor of two if other values of ϵ are assumed.

Regarding the $K^+ \rightarrow \mu^+ \nu_\mu Z' (\rightarrow e^+ e^-)$ decay, the constraints in the parameter space of the model are derived enforcing the hidden vector contribution to be smaller than the error bar in Eq.(39). In this case, we realize that the study of rare K^+ decays becomes quite fruitful, as seen in Fig.3. In both cases, with $\tan\beta = 10$ and $\tan\beta = 50$, the bounds we get from Kaon decays exclude a much larger region of parameter space than those from collider searches. In particular, for the $U(1)_{B-L}$ model we find $g_X < 2 \times 10^{-3}$ across the entire parameter space, while for the $U(1)_F$ model, $g_X < 5 \times 10^{-4}$. The constraints for the other models can be easily extracted from Fig.3 which resulted to be the most restrictive one.

In summary, we conclude that the $K^+ \rightarrow \mu^+ \nu_\mu Z' (\rightarrow \bar{\nu} \nu)$ rare decay does not lead to very restrictive bounds unless large values of $\tan\beta$ are adopted. Whereas, for $K^+ \rightarrow \mu^+ \nu_\mu Z' (\rightarrow e^+ e^-)$, which has a branching ratio over an order of magnitude smaller than the $K^+ \rightarrow \mu^+ \nu_\mu Z' (\rightarrow$

$\bar{\nu}\nu$), the probe of hidden vector becomes rewarding. For several $U(1)_X$ models, across the entire region of interest, the K^+ decay into $\mu^+\nu_\mu e^+e^-$ produces stronger limits than those from collider searches.

VI. CONCLUSIONS

Kaon mesons have played a key role in the construction of the Standard Model since their discovery in cosmic rays in 1947. They were of paramount importance to the understanding of the charged currents with the observation of the $K^+ \rightarrow \mu^+\bar{\nu}$ decay and were also essential in establishing the foundations of CP violation in 1964. Several studies to precisely measure the kaon decays have been conducted since then. Recently, a thousand of excess events were observed, leading to the measurement of the K^+ decay into $\mu^+\nu_\mu e^+e^-$. Motivated by this, we derived constraints on hidden vectors that belong to Abelian gauge symmetries in the context of Two Higgs Doublet Models. Our findings are based on rare K^+ decays into $\mu^+\bar{\nu}_\mu\nu\bar{\nu}$ and $\mu^+\bar{\nu}_\mu e^+e^-$.

Putting our results into perspective with other existing limits, we concluded that the most constraining rises from LEP searches for charged scalars. As the mass of the charged scalar is impacted by $\tan\beta$, we recast this limit as we explored different regions of the parameter space.

In summary, we found that the K^+ decay into $\mu^+\nu_\mu\nu\bar{\nu}$ rare decay is not very constraining, except when larger values of $\tan\beta$ are assumed. Nevertheless, the measurement of the $K^+ \rightarrow \mu^+\nu_\mu e^+e^-$ decay significantly improved the

power of probing hidden vectors. This decay model gave rise to the strongest limit for several $U(1)_X$ symmetries, for both $\tan\beta = 10$ and $\tan\beta = 50$. Conclusively, rare kaon decays constitute a great laboratory for probing light hidden particles.

ACKNOWLEDGMENTS

The authors thank Carlos Pires and Yoxara Villamizar for discussions. D.C thanks André de Gouvêa for the useful discussions, and motivation to develop this work. This work was financially supported by Simons Foundation (Award Number:1023171-RC), FAPESP Grant 2021/01089-1, ICTP-SAIFR FAPESP Grants 2021/14335-0, CNPq Grant 307130/2021-5, FONDECYT Grant 1191103 (Chile) and ANID-Programa Milenio-code ICN2019_044.

VII. APPENDIX

Here, we will obtain the interactions among fermions and the Z' field using the kinetic term,

$$\mathcal{L}_{\text{fermion}} = \sum_{\text{férmions}} \bar{\Psi}^L i\gamma^\mu D_\mu \Psi^L + \bar{\Psi}^R i\gamma^\mu D_\mu \Psi^R, \quad (41)$$

The covariant derivative must be written as a function of the physical neutral gauge bosons to then substitute it into Eq.(41). Doing so, and after a big algebra, we obtained for the left-handed fields,

$$\begin{aligned} \bar{\Psi}^L i\gamma^\mu D_\mu^L \Psi^L &= -eQ_f \bar{\psi}_f^L \gamma^\mu \psi_f^L A_\mu \\ &- \left[g_Z (T_{3f}^L - Q_f \sin^2 \theta_W) \cos \xi - \frac{1}{2} (\epsilon g_Z Q_{Yf}^L \tan \theta_W + g_X Q_{Xf}^L) \sin \xi \right] \bar{\psi}_f^L \gamma^\mu \psi_f^L Z_\mu \\ &- \left[g_Z (T_{3f}^L - Q_f \sin^2 \theta_W) \sin \xi + \frac{1}{2} (\epsilon g_Z Q_{Yf}^L \tan \theta_W + g_X Q_{Xf}^L) \cos \xi \right] \bar{\psi}_f^L \gamma^\mu \psi_f^L Z'_\mu, \end{aligned} \quad (42)$$

where were used the relations $g \sin \theta_W = g' \cos \theta_W = e$, $g_Z = g / \cos \theta_W$, $g' = g_Z \sin \theta_W$ and $T^3 + Q_Y/2 = Q$. As for the right-handed fields, it is enough to replace T_{3f}^L for

$T_{3f}^R = 0$ (actually, this is true for any field that transforms as a singlet by the SM symmetry regardless of its chirality), then,

$$\begin{aligned} \bar{\Psi}^R i\gamma^\mu D_\mu^R \Psi^R &= -eQ_f \bar{\psi}_f^R \gamma^\mu \psi_f^R A_\mu \\ &- \left[-g_Z Q_f \sin^2 \theta_W \cos \xi - \frac{1}{2} (\epsilon g_Z Q_{Yf}^R \tan \theta_W + g_X Q_{Xf}^R) \sin \xi \right] \bar{\psi}_f^R \gamma^\mu \psi_f^R Z_\mu \\ &- \left[-g_Z Q_f \sin^2 \theta_W \sin \xi + \frac{1}{2} (\epsilon g_Z Q_{Yf}^R \tan \theta_W + g_X Q_{Xf}^R) \cos \xi \right] \bar{\psi}_f^R \gamma^\mu \psi_f^R Z'_\mu. \end{aligned} \quad (43)$$

The sum of Eq.(42) and Eq.(43) accounts for the overall

interactions between left and right-handed fermions with the

physical neutral gauge bosons. It is useful to separate the con-

tributions for when $Q_{Xf}^{L,R} = 0$ and for $Q_{Xf}^{L,R} \neq 0$

$$\begin{aligned}
\mathcal{L} = & -eQ_f \bar{\psi}_f \gamma^\mu \psi_f A_\mu \\
& - \left[g_Z (T_{3f} - Q_f \sin^2 \theta_W) \cos \xi - \frac{1}{2} \epsilon g_Z Q_{Yf}^L \tan \theta_W \sin \xi \right] \bar{\psi}_f^L \gamma^\mu \psi_f^L Z_\mu \\
& - \left[-g_Z Q_f \sin^2 \theta_W \cos \xi - \frac{1}{2} \epsilon g_Z Q_{Yf}^R \tan \theta_W \sin \xi \right] \bar{\psi}_f^R \gamma^\mu \psi_f^R Z_\mu \\
& - \left[g_Z (T_{3f} - Q_f \sin^2 \theta_W) \sin \xi + \frac{1}{2} \epsilon g_Z Q_{Yf}^L \tan \theta_W \cos \xi \right] \bar{\psi}_f^L \gamma^\mu \psi_f^L Z'_\mu \\
& - \left[-g_Z Q_f \sin^2 \theta_W \sin \xi + \frac{1}{2} \epsilon g_Z Q_{Yf}^R \tan \theta_W \cos \xi \right] \bar{\psi}_f^R \gamma^\mu \psi_f^R Z'_\mu \\
& + \frac{1}{2} g_X Q_{Xf}^L \sin \xi \bar{\psi}_f^L \gamma^\mu \psi_f^L Z_\mu + \frac{1}{2} g_X Q_{Xf}^R \sin \xi \bar{\psi}_f^R \gamma^\mu \psi_f^R Z_\mu - \frac{1}{2} g_X Q_{Xf}^L \cos \xi \bar{\psi}_f^L \gamma^\mu \psi_f^L Z'_\mu \\
& - \frac{1}{2} g_X Q_{Xf}^R \cos \xi \bar{\psi}_f^R \gamma^\mu \psi_f^R Z'_\mu.
\end{aligned} \tag{44}$$

The last two lines of Eq.(44) are the contributions introduced when the charges of the fermions under $U(1)_X$ are non-zero. In the limit we are working, $M_{Z'} \ll M_Z$, i.e. with $\cos \xi \sim 1$, the interactions mediated by the standard Z boson are identical to the SM case, even in the case when $Q_{Xf}^{L,R} \neq 0$. Thus we get,

$$\mathcal{L}_Z = - (g_Z J_{NC}^\mu) Z_\mu. \tag{45}$$

For the Z' boson we have two contributions, the first one for when $Q_{Xf}^{L,R} = 0$,

$$\mathcal{L}_{Z'} = - (\epsilon e J_{em}^\mu + \epsilon_Z g_Z J_{NC}^\mu) Z'_\mu, \tag{46}$$

and a second one, which exists when $Q_{Xf}^{L,R} \neq 0$,

$$\mathcal{L}_{Z'} = - \left(\frac{1}{2} g_X Q_{Xf}^L \bar{\psi}_f^L \gamma^\mu \psi_f^L + \frac{1}{2} g_X Q_{Xf}^R \bar{\psi}_f^R \gamma^\mu \psi_f^R \right) Z'_\mu. \tag{47}$$

Notice that Eq.(46) represent the well-known DarK Z boson interactions, and its implications on parity violation, rare decays and Higgs physics have been studied in [50]. Moreover, when the mass mixing between the hidden boson and the Z boson is neglected in Eq.(46) ($\epsilon_z = 0$), we fall back to the Dark photon model, where the Z' couples to the SM particles proportionally to the kinetic mixing ϵe . Consequently, we are studying a more general version of the models already studied in the literature. The next and last step that we will take in this section is to write the interaction among the Z' boson and SM fermions in the form,

$$\mathcal{L}_{Z'}^{int} = g_V^{(\Psi_i)} \bar{\Psi}_i \not{Z}' \Psi_i + g_A^{(\Psi_i)} \bar{\Psi}_i \not{Z}' \gamma_5 \Psi_i, \tag{48}$$

with Ψ_i being each one of the fermions of the SM, g^V and g^A the vector and axial couplings which are set by the $U(1)_X$ charges, which characterizes each one of the anomaly free 2HDM- $U(1)_X$ models of the table I. Focusing on the charged leptons, Eq.(48) can be written as,

$$\mathcal{L}_{Z'} = \bar{e}_i \not{Z}' \left\{ \epsilon e + \frac{\epsilon_Z g_Z}{4} (1 - 4 \sin^2 \theta_W) + \frac{g_X}{8} (7u + 5d) + \left[-\frac{\epsilon_Z g_Z}{4} + \frac{g_X}{8} (u - d) \right] \gamma_5 \right\} e_i. \tag{49}$$

The corresponding lagrangian for the light neutrinos ν_i ($i = 1, 2, 3$) is,

$$\mathcal{L}_{Z'} = \bar{\nu}_i \not{Z}' \left\{ \frac{3g_X}{8} (u + d) - \frac{g_Z \epsilon_Z}{4} + \left[-\frac{3g_X}{8} (u + d) + \frac{g_Z \epsilon_Z}{4} \right] \gamma_5 \right\} \nu_i. \tag{50}$$

Lastly, for the quarks with positive and negative isospin, we find,

$$\mathcal{L}_{Z'} = \bar{u}_i \not{Z} \left\{ -\frac{2}{3} \epsilon e - \frac{\epsilon_Z g_Z}{4} \left(1 - \frac{8}{3} \sin^2 \theta_W \right) - \frac{g_X}{8} (3u + d) + \left[\frac{\epsilon_Z g_Z}{4} + \frac{g_X}{8} (d - u) \right] \gamma_5 \right\} u_i . \quad (51)$$

$$\mathcal{L}_{Z'} = \bar{d}_i \not{Z} \left\{ \frac{1}{3} \epsilon e + \frac{\epsilon_Z g_Z}{4} \left(1 - \frac{4}{3} \sin^2 \theta_W \right) - \frac{g_X}{8} (u + 3d) + \left[-\frac{\epsilon_Z g_Z}{4} + \frac{g_X}{8} (u - d) \right] \gamma_5 \right\} d_i . \quad (52)$$

With Eq.(49), Eq.(50), Eq.(51), and Eq.(52), we can derive the Z' branching ratio into any fermions. Using these equations,

we computed the total decay width as well as the branching ratio into neutrinos and e^+e^- .

-
- [1] G. Aad et al. (ATLAS Collaboration), *Phys.Lett.* **B716**, 1 (2012), [arXiv:1207.7214 \[hep-ex\]](#).
- [2] S. Chatrchyan et al. (CMS), *Phys. Lett. B* **716**, 30 (2012), [arXiv:1207.7235 \[hep-ex\]](#).
- [3] G. Van Onsem (ATLAS, CMS), in *57th Rencontres de Moriond on QCD and High Energy Interactions* (2023) [arXiv:2306.07677 \[hep-ex\]](#).
- [4] F. M. Simone (CMS), *Int. J. Mod. Phys. A* **37**, 2240003 (2022).
- [5] M. Aaboud et al. (ATLAS), *Phys. Rev. D* **98**, 092008 (2018), [arXiv:1807.06573 \[hep-ex\]](#).
- [6] G. Aad et al. (ATLAS), *Phys. Rev. Lett.* **127**, 271801 (2022), [arXiv:2105.12491 \[hep-ex\]](#).
- [7] G. Aad et al. (ATLAS), *Phys. Rev. Lett.* **129**, 061803 (2022), [arXiv:2201.13045 \[hep-ex\]](#).
- [8] T. D. Lee, *Phys. Rev. D* **8**, 1226 (1973).
- [9] H. E. Haber and G. L. Kane, *Phys. Rept.* **117**, 75 (1985).
- [10] N. Turok and J. Zadrozny, *Nucl. Phys. B* **358**, 471 (1991).
- [11] K. Funakubo, A. Kakuto, and K. Takenaga, *Prog. Theor. Phys.* **91**, 341 (1994), [arXiv:hep-ph/9310267](#).
- [12] A. T. Davies, C. D. Froggatt, G. Jenkins, and R. G. Moorhouse, *Phys. Lett. B* **336**, 464 (1994).
- [13] J. M. Cline, K. Kainulainen, and A. P. Vischer, *Phys. Rev. D* **54**, 2451 (1996), [arXiv:hep-ph/9506284](#).
- [14] S.-Q. Wang, X.-G. Wu, J.-M. Shen, H.-Y. Han, and Y. Ma, *Phys. Rev. D* **89**, 116001 (2014), [arXiv:1402.0975 \[hep-ph\]](#).
- [15] G. C. Branco, P. M. Ferreira, L. Lavoura, M. N. Rebelo, M. Sher, and J. P. Silva, *Phys. Rept.* **516**, 1 (2012), [arXiv:1106.0034 \[hep-ph\]](#).
- [16] J. Freund, G. Kreyerhoff, and R. Rodenberg, *Phys. Lett. B* **280**, 267 (1992).
- [17] J. Velinho, R. Santos, and A. Barroso, *Phys. Lett. B* **322**, 213 (1994).
- [18] S. Nie and M. Sher, *Phys. Lett. B* **449**, 89 (1999), [arXiv:hep-ph/9811234](#).
- [19] P. M. Ferreira, R. Santos, and A. Barroso, *Phys. Lett. B* **603**, 219 (2004), [Erratum: *Phys.Lett.B* 629, 114–114 (2005)], [arXiv:hep-ph/0406231](#).
- [20] R. A. Battye, G. D. Brawn, and A. Pilaftsis, *JHEP* **08**, 020 (2011), [arXiv:1106.3482 \[hep-ph\]](#).
- [21] X.-J. Xu, *Phys. Rev. D* **95**, 115019 (2017), [arXiv:1705.08965 \[hep-ph\]](#).
- [22] V. Branchina, F. Contino, and P. M. Ferreira, *JHEP* **11**, 107 (2018), [arXiv:1807.10802 \[hep-ph\]](#).
- [23] Y. Song, (2023), [arXiv:2301.09256 \[hep-ph\]](#).
- [24] M. Aoki, S. Kanemura, K. Tsumura, and K. Yagyu, *Phys. Rev. D* **80**, 015017 (2009), [arXiv:0902.4665 \[hep-ph\]](#).
- [25] Y. Bai, V. Barger, L. L. Everett, and G. Shaughnessy, *Phys. Rev. D* **87**, 115013 (2013), [arXiv:1210.4922 \[hep-ph\]](#).
- [26] A. Alves, D. A. Camargo, A. G. Dias, R. Longas, C. C. Nishi, and F. S. Queiroz, *JHEP* **10**, 015 (2016), [arXiv:1606.07086 \[hep-ph\]](#).
- [27] V. Barger, L. L. Everett, H. E. Logan, and G. Shaughnessy, *Phys. Rev. D* **88**, 115003 (2013), [arXiv:1308.0052 \[hep-ph\]](#).
- [28] B. Dumont, J. F. Gunion, Y. Jiang, and S. Kraml, *Phys. Rev. D* **90**, 035021 (2014), [arXiv:1405.3584 \[hep-ph\]](#).
- [29] M. Lindner, M. Platscher, and F. S. Queiroz, *Phys. Rept.* **731**, 1 (2018), [arXiv:1610.06587 \[hep-ph\]](#).
- [30] M. Misiak and M. Steinhauser, *Eur. Phys. J. C* **77**, 201 (2017), [arXiv:1702.04571 \[hep-ph\]](#).
- [31] P. Ko, Y. Omura, and C. Yu, *Phys. Lett. B* **717**, 202 (2012), [arXiv:1204.4588 \[hep-ph\]](#).
- [32] P. Ko, Y. Omura, and C. Yu, *JHEP* **01**, 016 (2014), [arXiv:1309.7156 \[hep-ph\]](#).
- [33] P. Ko, Y. Omura, and C. Yu, *JHEP* **11**, 054 (2014), [arXiv:1405.2138 \[hep-ph\]](#).
- [34] A. Crivellin, G. D'Ambrosio, and J. Heeck, *Phys. Rev. Lett.* **114**, 151801 (2015), [arXiv:1501.00993 \[hep-ph\]](#).
- [35] W.-C. Huang, Y.-L. S. Tsai, and T.-C. Yuan, *JHEP* **04**, 019 (2016), [arXiv:1512.00229 \[hep-ph\]](#).
- [36] W. Wang and Z.-L. Han, *Phys. Rev. D* **94**, 053015 (2016), [arXiv:1605.00239 \[hep-ph\]](#).
- [37] L. Delle Rose, S. Khalil, and S. Moretti, *Phys. Rev. D* **96**, 115024 (2017), [arXiv:1704.03436 \[hep-ph\]](#).
- [38] M. D. Campos, D. Cogollo, M. Lindner, T. Melo, F. S. Queiroz, and W. Rodejohann, *JHEP* **08**, 092 (2017), [arXiv:1705.05388 \[hep-ph\]](#).
- [39] D. A. Camargo, A. G. Dias, T. B. de Melo, and F. S. Queiroz, *JHEP* **04**, 129 (2019), [arXiv:1811.05488 \[hep-ph\]](#).
- [40] G. Arcadi, A. S. de Jesus, T. B. de Melo, F. S. Queiroz, and Y. S. Villamizar, *Nucl. Phys. B* **982**, 115882 (2022), [arXiv:2104.04456 \[hep-ph\]](#).
- [41] G. Arcadi, M. Lindner, J. Martins, and F. S. Queiroz, *Nucl. Phys. B* **959**, 115158 (2020), [arXiv:1906.04755 \[hep-ph\]](#).
- [42] Y. Mambrini, S. Profumo, and F. S. Queiroz, *Phys. Lett. B* **760**, 807 (2016), [arXiv:1508.06635 \[hep-ph\]](#).
- [43] D. A. Camargo, M. D. Campos, T. B. de Melo, and F. S.

- Queiroz, *Phys. Lett. B* **795**, 319 (2019), [arXiv:1901.05476 \[hep-ph\]](#).
- [44] P. Minkowski, *Phys. Lett.* **B67**, 421 (1977).
- [45] G. Lazarides, Q. Shafi, and C. Wetterich, *Nucl. Phys.* **B181**, 287 (1981).
- [46] R. N. Mohapatra and G. Senjanovic, *Phys. Rev. Lett.* **44**, 912 (1980).
- [47] R. N. Mohapatra and G. Senjanovic, *Phys. Rev.* **D23**, 165 (1981).
- [48] J. Schechter and J. W. F. Valle, *Phys. Rev.* **D22**, 2227 (1980).
- [49] B. Batell, M. Pospelov, and A. Ritz, *Phys. Rev. D* **83**, 054005 (2011), [arXiv:0911.4938 \[hep-ph\]](#).
- [50] H. Davoudiasl, H.-S. Lee, and W. J. Marciano, *Phys. Rev. D* **85**, 115019 (2012), [arXiv:1203.2947 \[hep-ph\]](#).
- [51] A. J. Buras, *JHEP* **04**, 071 (2016), [arXiv:1601.00005 \[hep-ph\]](#).
- [52] C.-W. Chiang and P.-Y. Tseng, *Phys. Lett. B* **767**, 289 (2017), [arXiv:1612.06985 \[hep-ph\]](#).
- [53] A. Crivellin, G. D'Ambrosio, M. Hoferichter, and L. C. Tunstall, *Phys. Rev. D* **93**, 074038 (2016), [arXiv:1601.00970 \[hep-ph\]](#).
- [54] K. S. Babu, C. F. Kolda, and J. March-Russell, *Phys. Rev. D* **57**, 6788 (1998), [arXiv:hep-ph/9710441](#).
- [55] P. Langacker, *Rev. Mod. Phys.* **81**, 1199 (2009), [arXiv:0801.1345 \[hep-ph\]](#).
- [56] S. Gopalakrishna, S. Jung, and J. D. Wells, *Phys. Rev. D* **78**, 055002 (2008), [arXiv:0801.3456 \[hep-ph\]](#).
- [57] G. Abbiendi et al. (ALEPH, DELPHI, L3, OPAL, LEP), *Eur. Phys. J. C* **73**, 2463 (2013), [arXiv:1301.6065 \[hep-ex\]](#).
- [58] D. A. Camargo, M. D. Campos, T. B. de Melo, and F. S. Queiroz, *Physics Letters B* **795**, 319 (2019).
- [59] R. L. Workman et al. (Particle Data Group), *PTEP* **2022**, 083C01 (2022).
- [60] M. Lindner, F. S. Queiroz, W. Rodejohann, and X.-J. Xu, *JHEP* **05**, 098 (2018), [arXiv:1803.00060 \[hep-ph\]](#).
- [61] A. Datta, A. Hammad, D. Marfatia, L. Mukherjee, and A. Rashed, *Journal of High Energy Physics* **2023** (2023), [10.1007/jhep03\(2023\)108](#).
- [62] E. C. Gil et al., *Physics Letters B* **816**, 136259 (2021).
- [63] A. A. Poblaguev et al., *Physical Review Letters* **89** (2002), [10.1103/physrevlett.89.061803](#).